3. NUCLEAR MODELS

The theory used to describe the deuteron nucleus is unpractical to be applied to heavy nuclei because from a mathematical point of view we should solve a many-body problem; furthermore such a microscopic approach could obscure the essential physics of the nucleus rather than facilitate its understanding. Therefore, the strategy is to construct simplified *nuclear models* that are mathematically tractable but at the same time allow to capture the essentials of nuclear physics.

3.1 The Shell Model

Nuclear physicists use a theory similar to the atomic physics shell model. However, the *nuclear shell model* contains fundamental differences. In the atomic case, the valence electrons experience a potential that is supplied by the Coulomb field of the nucleons, while in the nucleus, the nucleons move in a potential that they themselves create. Another difference consists in the fact that in the atomic shell theory the electrons can move in spatial orbits relatively free of collisions with other electrons, while nucleons are large compared to the size of the nucleus, thus it is hard to imagine them moving in orbits without making collisions with other nucleons.

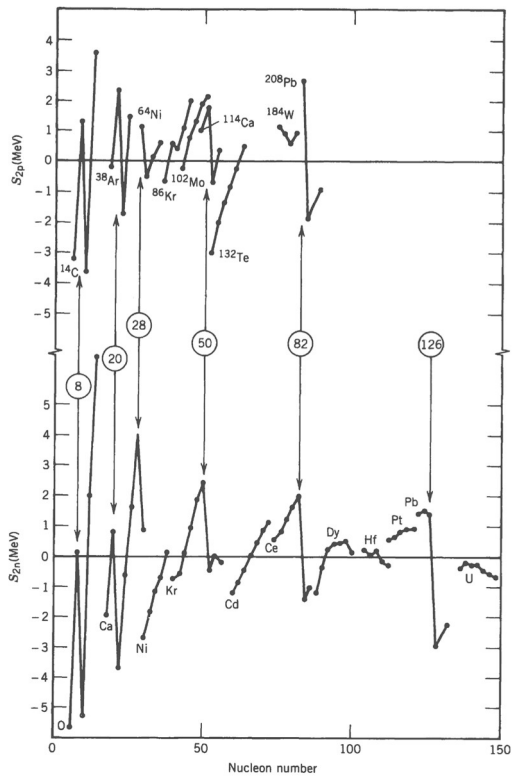

Figure 3.1 Two-proton separation energies of a sequence of isotones (top) and isotopes (bottom). The sudden change at the indicated "magic numbers" is clear (*from Krane*).

However, there are experimental evidences supporting the existence of nuclear shells. Fig.3.1 shows measured proton and neutron separation energies increasing gradually with N or Z except for a few sharp drops that occur at the same neutron and proton numbers. These so-called "magic-numbers" (Z or N = 2, 8, 20, 28, 50, 82, and 126) represent the effect of filled major shells.

The fundamental assumption of the shell model is that the motion of a single nucleon is governed by a potential caused by all the other nucleons. The existence of definite spatial orbits depends on the Pauli principle. Let us consider in a heavy nucleus a collision between two nucleons in a state near the very bottom of the potential well. When the nucleons collide, they will transfer energy to one another, but if all of the energy levels are filled up to the level of the valence nucleons, there is no way for one of the nucleons to gain energy except to move up to the valence level because the other levels (near the original one) are filled and cannot accept an additional nucleon. Such a transfer from a low-lying level to the valence band requires more energy than the nucleons are likely to transfer in a collision. Thus, the collisions cannot occur, and the shell model assumes that the nucleons orbit as if they were transparent to one another.

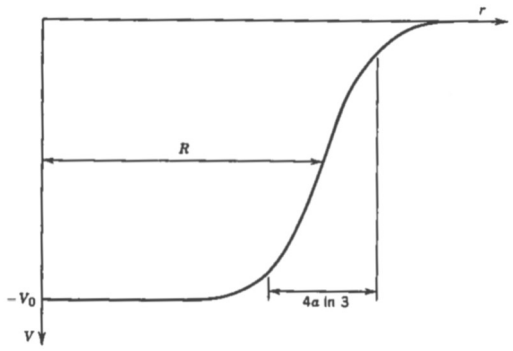

Figure 3.2 The shell-model potential (*from Krane*).

To develop this model, it is necessary to choose the ***shell-model potential***. The level degeneracy represents the number of nucleons that can be put in that level, namely *2(2L + 1)*. The factor of *(2L + 1)* arises from the m_L degeneracy, and the factor of *2* comes from the m_s degeneracy. In nuclear physics, the spectroscopic notation is different from the atomic physics one: the index *n* does not denote the principal quantum number, but simply counts the number of levels with a given *L* value. For instance, *1d* means the first (lowest) *d* state, *2d* means the second, and so on. A realistic form of the Shell model potential is sketched in Fig.3.2 and correspond to the following expression (*Woods-Saxon potential*):

$$V(r) = \frac{-V_0}{1+\exp\left(\frac{r-R}{a}\right)} \tag{3.1}$$

where R is the mean nuclear radius and a is the skin thickness: $R = 1.2 \cdot A^{1/3}$ *fm* and $a = 0.524$ *fm*, and the well depth V_0 is of the order of 50 MeV. The resulting energy levels are shown in Fig.3.3. Filling the shells with nucleons according to the $2(2L + 1)$ rule, allows to obtain the magic numbers 2, 8, and 20, but the higher magic numbers do not emerge from the calculations.

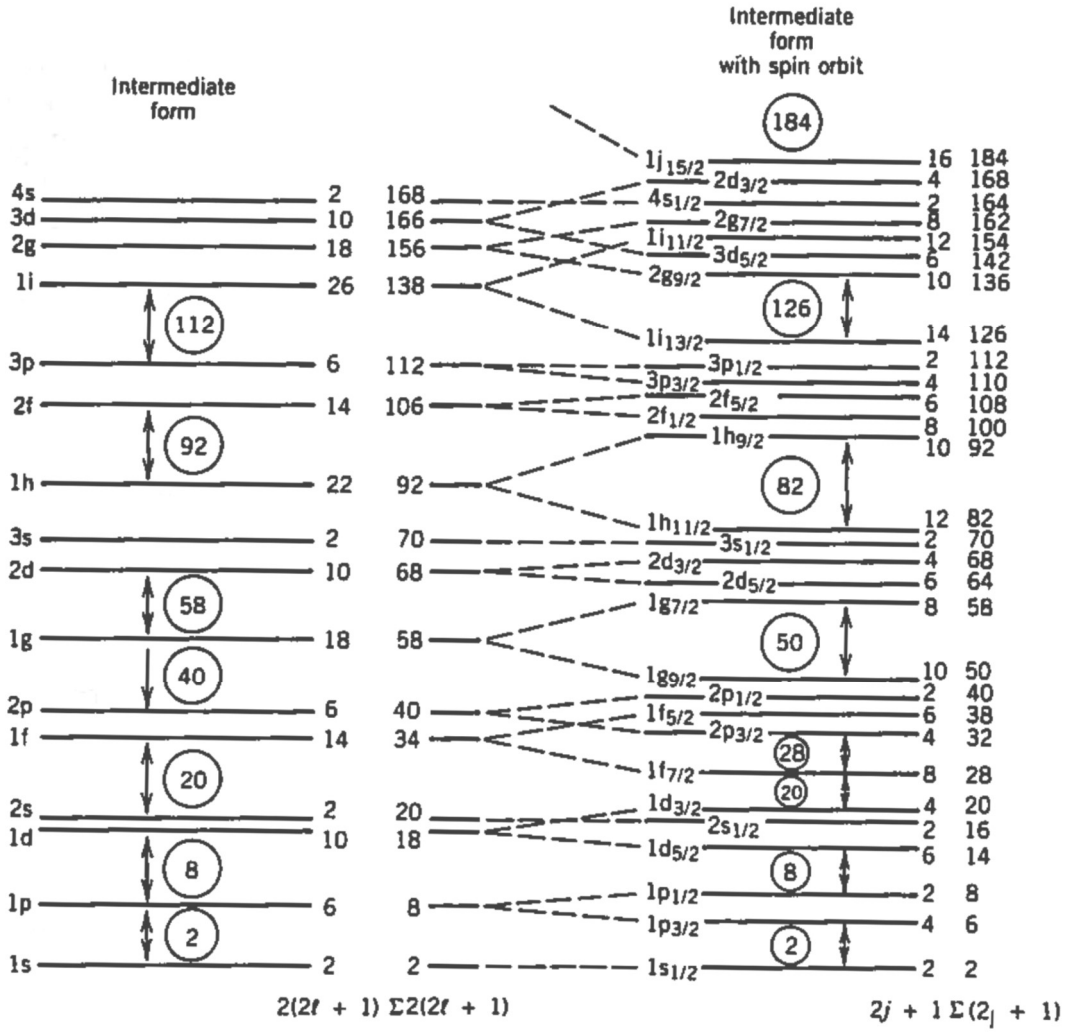

Figure 3.3 The shell-model energy levels without (left) and with (right) the spin orbit effect (*from Krane*).

Mayer, Haxel, Suess, and Jensen showed in 1949 that the inclusion of a **spin-orbit potential** could give the proper separation of the subshells and reproduce the magic numbers. The experimental evidence of a nucleon-nucleon spin-orbit force was already mentioned earlier. In the presence of a spin-orbit interaction it is appropriate to label the states with the total angular momentum $\boldsymbol{J} = \boldsymbol{L} + \boldsymbol{S}$. A single nucleon has $s = ½$, so the possible values of the total angular momentum quantum number are $J = L + ½$ *or* $J = L - ½$ (except for $L = 0$, in which case only $J = ½$ is allowed). Let us consider a level such as *1f* ($L = 3$), which has a degeneracy of $2(2L + 1) = 14$. The possible J values are $L \pm 1/2$, i.e. *5/2* or *7/2*; thus, we have the levels $1f_{5/2}$ and $1f_{7/2}$. The degeneracy of each level is $(2J + 1)$,

which comes from the m_J values. The capacity of the $1f_{5/2}$ level is therefore 6, and that of $1f_{7/2}$ is 8, giving again 14 states (the number of possible states must be preserved, but they are grouped differently). The $1f_{5/2}$ and $1f_{7/2}$ states are known as spin-orbit pair or doublet. Considering the spin-orbit effect allows to obtain the remaining magic numbers as expected. Fig.3.4 shows a typical example of application of the shell model, considering the filling of energy levels needed to produce $^{15}_{8}O$ and $^{17}_{8}O$. The 8 protons fill a major shell and do not contribute to the structure. The extreme limit of the shell model claims that only the single unpaired nucleon determines the properties of the nucleus. In the case of $^{15}_{8}O$ the unpaired nucleon is in the shell $1p_{1/2}$; therefore we would predict that the ground state of $^{15}_{8}O$ has spin ½ and odd parity (*L=1*), since the parity is determined by $(-1)^L$. Similarly, the ground state of $^{17}_{8}O$ should have spin 5/2 and even parity (*L=2*), since the unpaired nucleon is in the $1d_{5/2}$ level. These two predictions are in perfect agreement with the observed spin-parity assignments.

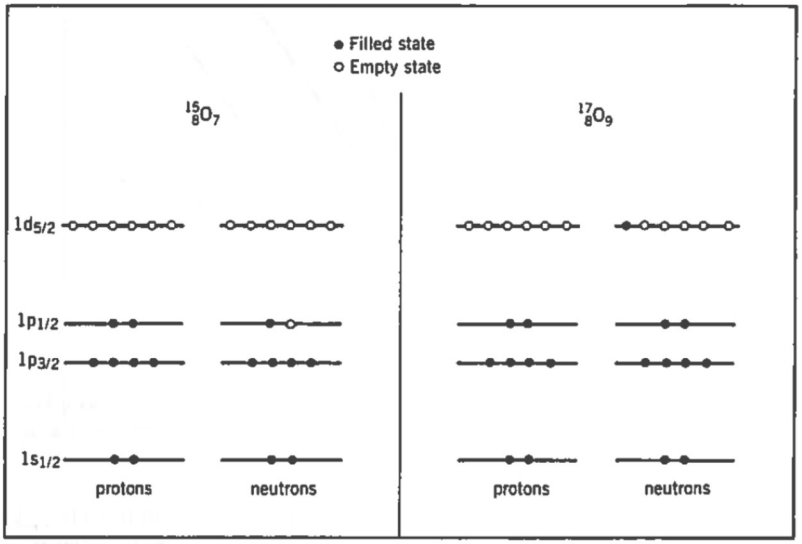

Figure 3.4 The filling of shells in ^{15}O and ^{17}O (*from Krane*).

In the case of **magnetic dipole moments**, the shell model still gives a reasonable (but not exact) agreement with experimentally measured nuclear properties. The magnetic moment is calculated from the expectation value of the magnetic moment operator in the state with maximum z projection of angular momentum. Including both *L* and *S* terms, we can express it as:

$$\mu = \frac{\mu_N (g_L L_z + g_S S_z)}{\hbar} \tag{3.2}$$

where $g_L = +1$ for a proton, $g_L = 0$ for a neutron, $g_S = +5.5856$ for a proton, and $g_S = -3.8262$ for a neutron. According to the Shell Model, for odd-*A* nuclei we expect $\langle\mu\rangle \neq 0$, and it can be expressed as follows:

$$\langle\mu\rangle = \left[g_L\left(J-\frac{1}{2}\right)+\frac{1}{2g_S}\right]\mu_N \qquad J = L+\frac{1}{2}$$

$$\langle\mu\rangle = \left[g_L\frac{J(J+3/2)}{J+1} - 1/2\,\frac{1}{J+1}g_S\right]\mu_N \qquad J = L-1/2 \qquad (3.3)$$

Fig.3.5 shows a comparison of calculated values of the of magnetic moments, using the shell-model for odd-A nuclei (known as Schmidt lines), and experimental measurements. The experimental data are generally smaller in magnitude and show a large scatter. The main reason for such disagreement lies in the oversimplified assumption that g_S for a nucleon in a nucleus is the same as g_S for a free nucleon. This is not a surprising effect if one considers that the "meson cloud" surrounding a free nucleon differs from the meson cloud of a nucleon bounded within the nucleus. Typically, this effect is considered by arbitrary reducing the g_S factor (e.g. 0.6 g_S in Fig.3.5). However the scattering of the experimental point is still large and suggests that the shell-model theory oversimplifies the calculation of the magnetic moments.

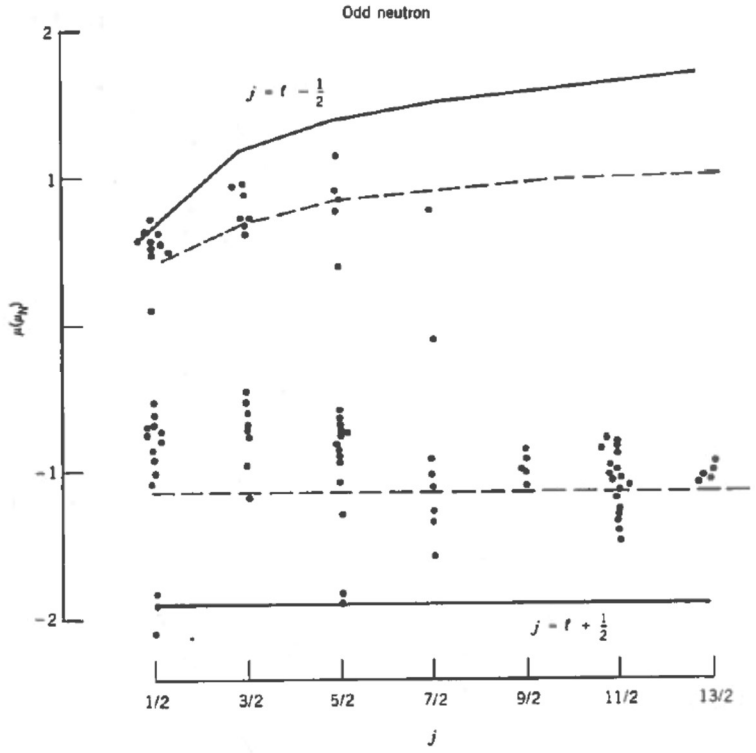

Figure 3.5 Experimental (dots) and calculated (line) values of the magnetic moments of odd-A nuclei. The Schmidt lines are shown as solid for g_s (free nucleons) and dashed for 0.6g_s (*from Krane*).

The computation of **electric quadrupole moments** in the shell-model is done by evaluating the electric quadrupole operator, $3z^2 - r^2$, in a state in which the total angular momentum of the odd particle has its maximum projection along the *z* axis (i.e. $m_J = +J$). Assuming that the odd particle is a proton, and that its angular momentum is aligned with the *z* axis, then it must be orbiting in the *xy* plane ($z = 0$). This would give a negative quadrupole moment of the order of $Q = -\langle r^2\rangle$.

Calculated values are in good agreement with expectations, although a more accurate quantum mechanical computation gives the single-particle quadrupole moment of an odd proton in the state *J* of the shell-model as:

$$\langle Q_{sp} \rangle = -\frac{2J-1}{2(J+1)} \langle r^2 \rangle \tag{3.4}$$

where $\langle r^2 \rangle = 3/5R^2 = 3/5R_0^2A^{2/3}$.

A less intuitive case is the one of an odd neutron. In fact, one would expect no quadrupole moment for an uncharged particle outside a filled subshell. However, odd-neutron values are not zero, even if they are generally smaller than the odd-proton case. When a subshell contains more than a single particle, all the particles in the subshell can contribute to the quadrupole moment. Since the capacity of a subshell is *2J + 1*, the number of nucleons in an unfilled subshell will range from *1* to *2J*. In this case, the quadrupole moment can be expressed as follows:

$$\langle Q \rangle = \langle Q_{sp} \rangle \left[1 - 2\frac{n-1}{2J-1}\right] \tag{3.5}$$

where *n* is the number of nucleons in the subshell ($1 \leq n \leq 2J$). When $n = 2J$ (subshell lacking only one nucleon from being filled), $Q = -Q_{sp}$. These are known as "hole" states and show positive and opposite (in sign) values of the quadrupole moment compared to the "particle" states. However, the model fails to predict the extremely large quadrupole moments of certain heavy nuclei. A proper explanation requires the use of theoretical models that are different from the shell-model. Nevertheless, despite its simplicity, the shell-model is successful in accounting for the spins and parity of nearly all odd-A ground states.

3.3 The Liquid Drop Model

The liquid drop model is based on two properties that are common to all nuclei (except small-A nuclei): (i) their interior mass densities are approximately the same, and (ii) their total binding energies are proportional to their masses (B/A ≈ constant). Both properties are compatible to the ones of macroscopic drops of an incompressible liquid: (i) the interior densities are constant, and (ii) the heats of vaporization (energy required to disperse the drop) are proportional to the masses. The liquid drop model approximates the nucleus as a sphere with a uniform interior density, abruptly dropping to zero at its surface. The radius is proportional to $A^{1/3}$, the surface area to $A^{2/3}$, and the volume to *A*. The mass formula consists of a sum of six terms:

$$\boxed{M_{Z,A} = f_0(Z,A) + f_1(Z,A) + f_2(Z,A) + f_3(Z,A) + f_4(Z,A) + f_5(Z,A)} \tag{3.6}$$

where $M_{Z,A}$ represents the mass of an atom whose nucleus is specified by Z and A. The first term is the mass of the constituent parts of the atom:

$$f_0(Z,A) = 1.007825\,Z + 1.008665\,(A-Z) \tag{3.7}$$

The remaining terms correct for the mass equivalents of various effects contributing to the total nuclear binding energy. The volume term is:

$$f_1(Z,A) = -a_1 A \tag{3.8}$$

This term describes the tendency to have a constant binding energy per nucleon, and since it is negative, it reduces the mass and increases the binding energy. The surface term is:

$$f_2(Z,A) = a_2 A^{2/3} \tag{3.9}$$

that represents a correction for the surface area of the nucleus. This term is positive, thus increases the mass and reduces the binding energy. In analogy with a liquid drop, this term would represent the effect of the surface tension energy. In fact, a molecule at the surface of the drop feels attractive forces only from one side, thus its binding energy is less than the binding energy of a molecule in the interior which feels attractive forces from all sides. The Coulomb term is:

$$f_3(Z,A) = a_3 \frac{Z^2}{A^{1/3}} \tag{3.10}$$

This term accounts for the effect of the Coulomb repulsion between the protons, thus increases the mass and reduces the binding energy. The next one is the asymmetry term:

$$f_4(Z,A) = a_4 \frac{(Z-\frac{A}{2})^2}{A} \tag{3.11}$$

which accounts for the tendency to have $Z = N$. This term is zero for $Z = N$, but increases with increasing departure from this condition, thus increases the mass and reduces the binding energy. Finally, the pairing term accounts for the tendency of nuclei to have even Z and even N:

$$\begin{aligned} f_5(Z,A) &= -a_5 A^{-\frac{1}{2}} && (Z\ even\ and\ N\ even) \\ f_5(Z,A) &= 0 && (Z\ even\ and\ N\ odd, or\ N\ even\ and\ Z\ odd) \\ f_5(Z,A) &= a_5 A^{-\frac{1}{2}} && (Z\ odd, N\ odd) \end{aligned} \tag{3.12}$$

This term maximises the binding energy if both Z and N are even.

Eq. (3.6) is known as *semiempirical mass formula* because the parameters a_1 to a_5 are obtained by empirically fitting the measured masses. One set of such parameters which provides accurate results for all stable nuclei, except very small A, is the following: $a_1 = 0.001691$; $a_2 = 0.001911$; $a_3 = 0.000763$; $a_4 = 0.10175$; $a_5 = 0.012$.

3.3 The Collective Model

The collective model of the nucleus combines certain features of the shell and liquid drop models. The collective model assumes that the nucleons in unfilled subshells of a nucleus move independently in a net nuclear potential produced by the *core* of filled subshells, as in the shell model. However, the net potential due to the core is not the static spherical symmetrical potential V(r) used in the shell model, but it is a potential capable undergoing deformations in shape. These deformations represent the collective motion of the nucleons that are associated with the liquid drop model. As in the shell model, the nucleons fill the energy levels corresponding to such potential, which are split by the same spin-orbit interaction and lead to the same magic numbers, as well as nuclear spin and parity predictions.

There are general properties that are common to all nuclei, and it is reasonable to identify those properties not with the motion of a few valence nucleons, but instead with the entire nucleus. The origin of such properties lies in the nuclear collective motion. Fig.3.6 shows properties of even-even nuclei that reveal collective behaviour. The energy of the first 2^+ excited state seems to decrease rather smoothly as a function of *A* (except in regions near the filled subshells). The region from about $A = 150$ to $A = 190$ shows value of $E(2^+)$ that are very small and constant. Fig.3.7 shows the magnetic moments of the 2^+ states that are fairly constant in the range *0.7-1.0*. In general, the observed nuclear properties suggest that it is convenient to consider two types of collective structures, for the nuclei with $A < 150$, and for the nuclei with $150 < A < 190$. The nuclei with $A < 150$ are typically treated in terms of a model based on vibrations about a spherical equilibrium shape, while the nuclei with $150 < A < 190$ are show structures most characteristic of rotations of a non-spherical system. Vibrations and rotations are the two major types of collective nuclear motion. This is treated with a similar mathematical approach used in the liquid drop model.

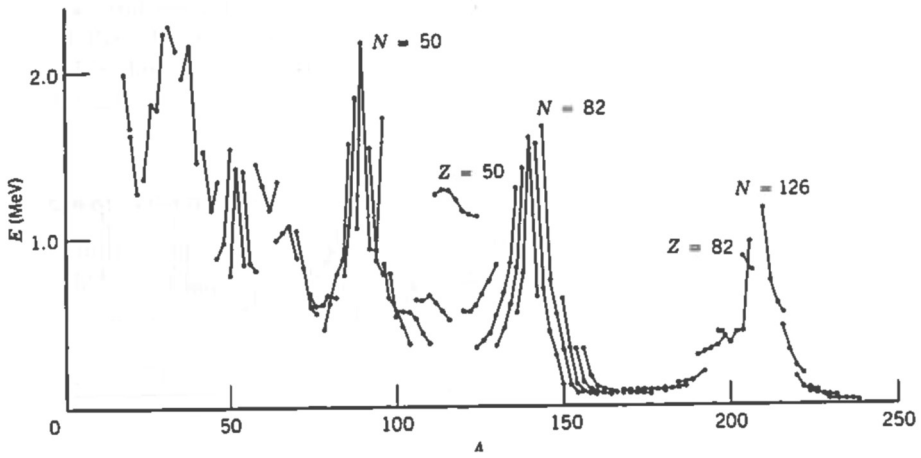

Figure 3.6 Energies of lowest 2^+ states of even-Z, even-N nuclei (*from Krane*).

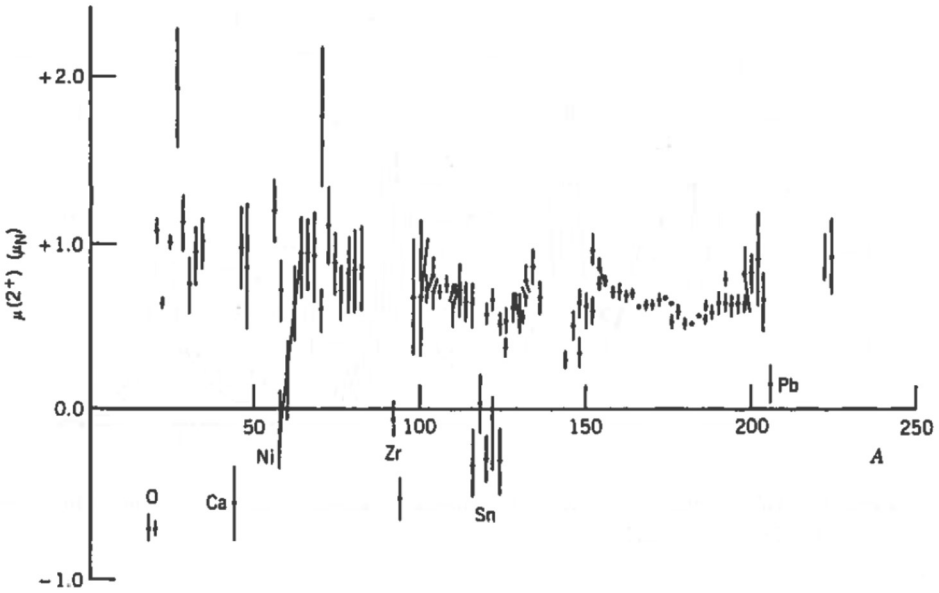

Figure 3.7 Magnetic moments of lowest 2^+ states of even-Z, even-N nuclei (*from Krane*).

Although the average shape of the nucleus is spherical, its instantaneous shape is not due to **nuclear vibrations**. It is convenient to define the position of a point on the nuclear surface using spherical (instantaneous) coordinates, *R(t)* and *(θ, ϕ)*, as shown in Fig.3.8, in terms of the spherical harmonics $Y_{L,m}(\theta, \phi)$. Each spherical harmonic component will have an amplitude $\alpha_{L,m}(\theta, \phi)$:

$$R(t) = R_{av} + \sum_{L\geq 1} \sum_{m=-L}^{+L} \alpha_{Lm}(t) Y_{Lm}(\theta, \varphi) \qquad (3.13)$$

The constant (*L = 0*) term is incorporated into the average radius R_{av}, which is just $R_0 A^{1/3}$.

The *L = 1* vibration is known as *dipole vibration*, as shown in Fig.3.9. This gives a net displacement of the centre of mass, and therefore cannot result from the action of internal nuclear forces. The next lowest mode is the *L = 2* vibration known as *quadrupole vibration* (see Fig.3.9).

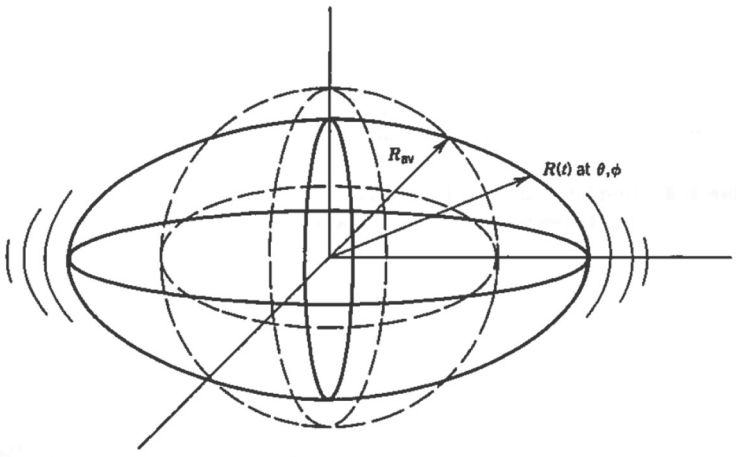

Figure 3.8 Representation of a vibrating nucleus with a spherical equilibrium shape. The time dependant coordinate *R(t)* defines a point on the surface in the direction *(θ, ϕ)* (*from Krane*).

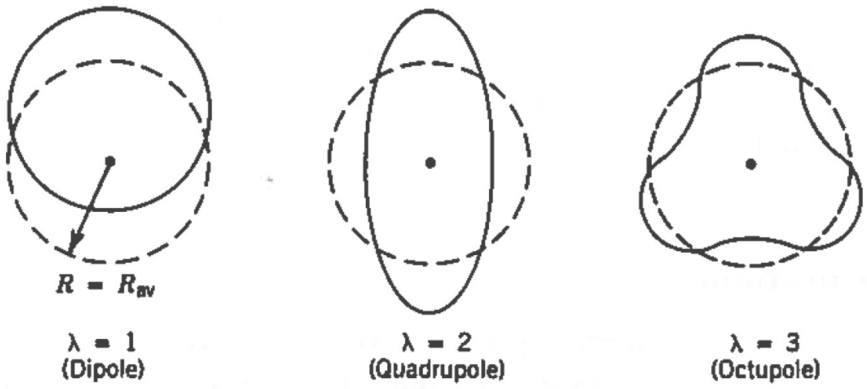

Figure 3.9 The lowest three vibrational modes of a nucleus. The dashed lines show the spherical equilibrium shape and the solid lines show an instantaneous view of the vibrating surfaces (*from Krane*).

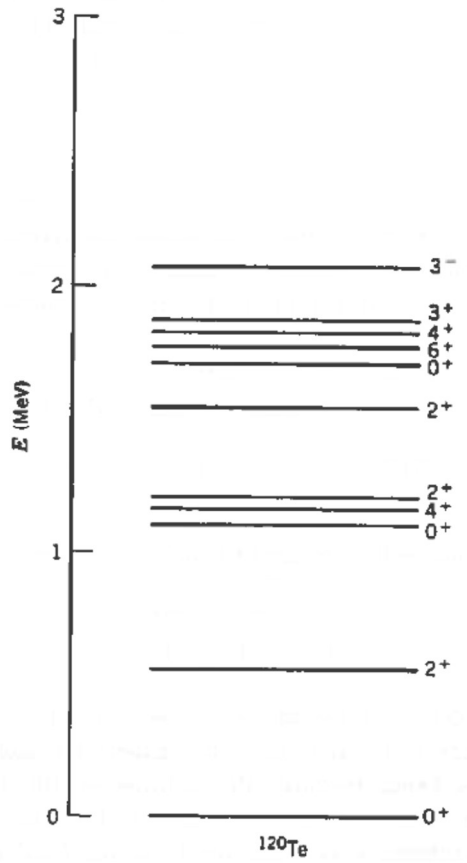

Figure 3.10 The low-lying levels of ^{120}Te (*from Krane*).

In analogy with the quantum theory of electromagnetism, in which a unit of electromagnetic energy is called photon, a quantum vibrational energy is called *phonon*. Thus, producing a mechanical vibration is equivalent to producing vibrational phonons. A single unit of $L = 2$ nuclear vibration is thus a *quadrupole phonon*. Let us consider the effect of adding one unit of vibrational energy (a quadrupole phonon) to the 0^+ ground state of an even-even nucleus. The $L = 2$ phonon carries 2 units of angular momentum and even parity (since the parity of $Y_{L,m}$ is $(-1)^L$). Thus, adding

two units of angular momentum to a 0^+ state gives only a 2^+ state, in perfect agreement with the measured spin-parity of first excited states of spherical even-Z, even-N nuclei. Let us assume to add an additional quadrupole phonon. We expect a triplet of states with spins 0^+, 2^+, 4^+ (*L=0, L=2, L=4*, respectively) at twice the energy of the first 2^+ state, since two identical phonons carry twice as much energy as one. The next highest mode of vibration is known as *octupole vibration* mode and corresponds to *L = 3* (see Fig.3.9). This mode carries three units of angular momentum and negative parity. Adding a single octupole phonon to the 0^+ ground state gives a 3^- state. Such states are commonly found at energies above the two-phonon triplet. An example of the vibrational states discussed above is reported in Fig. 3.10 for ^{120}Te.

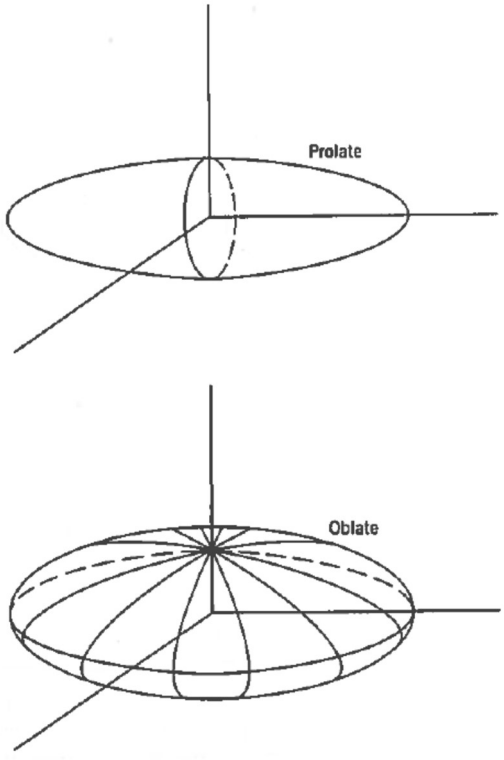

Figure 3.11 Equilibrium (static) shapes of deformed nuclei (*from Krane*).

Nuclei with non-spherical equilibrium shape can show **nuclear rotation** motion. These nuclei can have substantial distortions from spherical shape and are known as *deformed nuclei*. Their mass is in the range *150 < A < 190*, and *A > 220* (rare earths and actinides). These nuclei are usually represented as an ellipsoid of revolution (see Fig.3.11). Their surface can be described as follows:

$$R(\theta,\varphi) = R_{av}[1 + \beta Y(\theta,\varphi)] \tag{3.14}$$

The deformation parameter β is related to the eccentricity of the ellipse:

$$\beta = \frac{4}{3}\sqrt{\frac{\pi}{5}}\frac{\Delta R}{R_{av}} \tag{3.15}$$

where ΔR is the difference between the semimajor and the semiminor axes of the ellipse. When $\beta > 0$, the nucleus has the elongated form of a *prolate* ellipsoid, while $\beta < 0$ implies that the nucleus has the flattened form of an *oblate* ellipsoid.

One indicator of stable deformation of a nucleus is a large *electric quadrupole moment*. Let us assume that the nucleus is rotating in the laboratory frame of reference. The kinetic energy of a rotating object is $\frac{1}{2}\mathfrak{I}\omega^2$, where $\mathfrak{I}$ is the moment of inertia. In terms of angular momentum $L = \mathfrak{I}\omega^2$, the energy is $L^2/2\mathfrak{I}$. Taking the quantum mechanical value of L^2, and letting I represent the angular momentum quantum number of the nucleus, gives:

$$E = \frac{\hbar^2}{2\mathfrak{I}} I(I+1) \tag{3.16}$$

for the energies of a rotating object in quantum mechanics. Increasing the quantum number I corresponds to adding rotational energy to the nucleus, and the nuclear excited states form a sequence known as *rotational band*. The ground state of an even-Z, even-N nucleus is always a 0^+ state, and the mirror symmetry of the nucleus restricts the sequence of rotational states in this special case to even values of *I*. Therefore, we expect to see the following sequence of states: $E(0^+) = 0$; $E(2^+) = 6(\hbar^2/2\mathfrak{I})$; $E(4^+) = 20(\hbar^2/2\mathfrak{I})$; $E(6^+) = 42(\hbar^2/2\mathfrak{I})$; $E(8^+) = 72(\hbar^2/2\mathfrak{I})$; and so on. Indication of the lack of rigidity of a nucleus is the increase in the moment of inertia occurring at high angular momentum or rotational frequency. This effect is known as *centrifugal stretching* and is observed most often in heavy-ion reactions. In fact, the nucleus has no "vessel" to define the shape of the rotating fluid, and it is the potential provided by the nucleons themselves giving the nucleus its actual shape.

Both the vibrational and rotational collective motions give the nucleus a *magnetic moment* based on the corresponding angular momentum *I*:

$$\mu(I) = I\frac{Z}{A}\mu_N \tag{3.17}$$

For light nuclei, $Z/A \approx 0.5$ and $\mu(2) \approx +1\mu_N$, while for heavier nuclei, $Z/A \approx 0.4$ and $\mu(2) \approx +0.8\mu_N$.